Journal of Applied and Computational Mechanics

Research Paper

Finite Element Modelling and Simulation of the Hysteretic Behaviour of Single- and Bi-metal Cantilever Beams using a Modified Non-linear Beta-damping Model

H.B. Tariq[1], C. Rajakumar[2], D. Zhang[3], C. Spitas[4]

[1] Department of Mechanical and Aerospace Engineering, Nazarbayev University, Qabanbay Batyr 53, Nur-Sultan, 010000, Kazakhstan, Email: hamza.tariq@nu.edu.kz

[2] Department of Mechanical and Aerospace Engineering, Nazarbayev University, Qabanbay Batyr 53, Nur-Sultan, 010000, Kazakhstan, Email: crajakumar@yahoo.com

[3] Department of Civil and Environmental Engineering, Nazarbayev University, Qabanbay Batyr 53, Nur-Sultan, 010000, Kazakhstan, Email: dichuan.zhang@nu.edu.kz

[4] Department of Mechanical and Aerospace Engineering, Nazarbayev University, Qabanbay Batyr 53, Nur-Sultan, 010000, Kazakhstan, Email: cspitas@gmail.com

Abstract. This paper explores a novel non-linear hysteresis model obtained from the modification of the conventional Kelvin-Voigt model, to produce a non-viscous hysteretic behaviour that is closer to metal damping. Two case studies are carried out for a vibrating cantilever beam under tip loading (bending), the first considering a single uniform material and the second considering a bimetallic structure. The damping behaviour is studied in the frequency domain (constant damping ratio model vs. Kelvin-Voigt/ beta damping model) and time-domain (proposed modified hysteresis model vs. Kelvin-Voigt/ beta damping model). In the frequency domain, it was found that the Kelvin-Voigt model essentially damps out the displacement response of the modes more than the constant damping ratio model does. In the transient analysis, the Kelvin-Voigt model likewise produced unnaturally rapid damping of the oscillations for both the single- and bi-metal beam, compared to the modified hysteretic damping model, which produced a damping behaviour closer to actual metal behaviour. This was consistent with results obtained in the frequency domain.

Keywords: Hysteretic damping; Kelvin-Voigt model; beta-damping; finite element analysis; time-domain.

1. Introduction

For any structural system, a vital component for understanding dynamic behaviour is damping which, leads to energy dissipation during vibration [1-4]. The importance of damping is widely recognised in engineering dynamics. It is combined into numerical analysis by various damping models, which links the damping forces to the motions of the system's degrees of freedom (DOFs).

The most common model, the Kelvin-Voigt model, is applicable to viscous damping, where the damping element generates a force that is directly proportional to the velocity of response [1]. This model despite its simplicity is not suitable for solid materials, as it suggests that the energy dissipated in one harmonic cycle is proportional to the vibration frequency. Practical observations of mechanical and solid structural systems also imply a lack of systematic dependence of energy dissipation on frequency [2]. It is widely known that for such structures, for example, metallic structures, the energy dissipated per cycle is a result of factors such as localized plastic deformation, microscopic internal friction or plastic flow, which are some of the major contributors of energy dissipation in such systems, as a result, these systems are not sensitive to velocity, hence a viscous damping model is not applicable [4-7]. This led to the introduction of a frequency-independent damping model called the hysteresis damping model.

Kimball and Lovell [8] introduced the concept of frequency-independent damping as they discovered many engineering materials that displayed internal damping (independent of frequency), in which energy loss per cycle is proportional to the square of the strain amplitude. Their basic idea was to modify the viscous damping model so that the resulting dissipating energy is independent of frequency. Later a change was reported in Bishop's [9] article in which the time-domain equation of motion was modified by substituting viscous damping coefficient with another one that is inversely proportional to the harmonic forcing frequency. This then led other researchers to consider the equivalent frequency-domain equation of motion which then appeared to have a complex stiffness term [9-12]. This complex stiffness model was considered equivalent to the hysteretic model for all cases including the free vibration case [13].

This initiated debates on whether the structural hysteresis model (complex form) violates the causality principle. Some researchers [11,14-15] discovered from the impulse response functions for systems with hysteresis damping that the ideal hysteresis damper violates the requirement of causality. This is due to the response of the hysteresis damper before excitation. For many applications, this non-physical behaviour of the model is not a fatal flaw, for instance in stationary random vibration.

Researchers then tried to find a solution to the non-causality effect [16]. Some utilized convolution integrals of motion [17-20] others manipulated Hilbert transform to achieve causal hysteretic damping [21]. Besides, the quasi-hysteretic model was developed that relied on the correction of the dissipated energy at each time step that is from the complete prior motion history [22-23]. The issue with all these models is that they require extensive computation and information on the complete previous vibration history. This is not feasible in the context of when a single-degree-of-freedom (SDOF) model is generalised to multiple degrees of freedom (MDOF). Some researcher believed that causality is caused due to its wrong application and the assumption of the damping ratio is constant and real [24].

In finite element applications, there are three methods for damping modelling: Complex Eigenvalue (CE), Direct Frequency Response (DFR) and Modal Strain Energy (MSE) methods [25]. In the CE method, simplified assumptions cannot be made when solving a complex eigenvalue problem. Though this method is recognised for its estimation of structures damping levels, in practice it does have its imperfection [26]. In the DRF method, the inversion of the dynamic stiffness matrix is required for the determination of the FRF matrix, from which damping values can be evaluated. This method however is expensive due to its high computation time. In the MSE model, the approximation of modal damping levels is done with the Normal Modal Analysis of the undamped system with the computation of strain energy ratios for individual mode. In this method, the actual damped system eigenvalue problem is not solved. The MSE method assumptions limit its application for general use, even though it can be utilised for modelling complex damped structures.

The finite element methods discussed thus far is capable of modelling the composite structure damping and carrying out modal analysis that allows the structures complex mode shapes to be determined directly from the complex eigenvalue problem solution [27-31]. However, it should be noted that currently there are still no accurate and reliable damping estimation tools present in the finite element packages. Thus, a more robust model is needed, that will produce reliable results irrespective of the excitation frequency and will not require specific calibration of the model parameters, as is required by the Kelvin-Voigt family of models, including beta-damping.

In this paper, we have developed a finite element MDOF hysteresis model that is based on its instantaneous state under forced vibration that does not require prior knowledge of the history of motion, excitation characteristics and frequency. This model was first introduced very recently for the SDOF system by Spitas et al. [32] and is herein expanded to the MDOF problem, in consideration of multiple material domains. The model introduces a local correction factor, having the magnitude of an instantaneous frequency, computed based on the system local state variables at each time step. In the transient analysis, this model will be applied on a cantilever beam and its response will be compared with the conventional Kelvin-Voigt/ beta-damping model. Also, harmonic sweep analysis will be conducted to compare the responses from the constant damping ratio model (which is approximately the frequency-domain equivalent of the proposed model) and the Kelvin-Voigt model.

2. Theoretical models for structural hysteresis: Multi DOF FEA Models

2.1 Rayleigh damping

As discussed before, the Rayleigh damping model [33] is the combination of stiffness and mass proportional viscous damping and results in symmetric viscous system damping matrix for finite element multi-degree of freedom system.

$$\mathbf{C} = \alpha \mathbf{M} + \beta \mathbf{K} \tag{1}$$

The EOM for free viscously damped vibration of a structure is:

$$\mathbf{K}u + \mathbf{C}\dot{u} + \mathbf{M}\ddot{u} = 0 \tag{2}$$

where $\mathbf{K}$, $\mathbf{C}$, and $\mathbf{M}$ are stiffness, damping, and mass matrices (all real and constant), u is the vector of nodal displacement, $\dot{u}$ and $\ddot{u}$ are its first- and second-order time derivatives.

The eigenvalue solution can be obtained in terms of damped normal modes [34]. The method is quite standard as the modes obey the orthogonality condition, despite both eigenvectors and eigenvalues being complex, thus obtaining uncoupled equations of motion.

The complex eigenvalue method has two noticeable drawbacks. The first being its computational cost as it is three times the cost of undamped eigen-solution [35]. Also, materials must exhibit dynamic stress-strain behaviour of a certain type, for the structure to be described by EOM. The loss moduli have to increase with frequency and the storage moduli are constant [12]. However, real viscoelastic material does not behave in this way as the loss factor exhibit a single mild peak and the storage moduli tend to increase with frequency monotonically [4, 35].

2.2 Stiffness proportional structural damping

For ductile elastic materials like metal and steel, viscoelastic behaviour assumption is often insufficient for internal damping. On the contrary, for harmonic forced vibration, the damping ratio is shown to be free from forcing frequency Ω [36]. This can be demonstrated from the substitution of the loss factor $g_{s,v}$ (stiffness proportional viscous damping) with:

$$g_{s,v} = \frac{g_{s,s}}{\Omega} \tag{3}$$

where $g_{s,s}$ is the loss factor of stiffness proportional to structural damping. The model is only valid in the frequency domain for stationary harmonic vibration at a specific frequency Ω. Non-casual behaviour can be observed in the time domain if a non-harmonic dynamic load is applied.

The modal damping ratio, D, is constant, considering that the loaded structure responds with $u(t) = \hat{u}e^{-i\omega_u t}$, where $\omega_u = \Omega$ is the undamped frequency.

$$D = \frac{1}{2}g_{s,s}\frac{\omega_u}{\Omega} \approx \frac{1}{2}g_{s,s} = constant \tag{4}$$

The EOM changes to:

$$\mathbf{M}\ddot{u} + \mathbf{K^c}u = 0 \tag{5}$$

in which, the stiffness matrix $\mathbf{K^c} \epsilon \mathbb{C}$, i.e. $\mathbf{K^c} = \mathbf{K}(1 + ig_{s,s}) = \mathbf{K} + i\mathbf{C}$. The complex eigenvalue solution can still be obtained and gives n pair of complex eigenvalues $\lambda_{n1/n2} = \pm i\omega_{0,n}(1 + i2D_n)$. As a result of the stiffness proportionality of $\mathbf{C}$, the undamped

neighbouring system is the same as n eigenvectors.

When this stiffness model is employed, the damping term in the EOM will result in a complex dynamic stiffness matrix, which then leads to complex transcend

There are several disadvantages to using this method. As with the previous method, it computationally expensive due to the requirement of the displacement impedance matrix for a general sinusoidal solution, to be decomposed, recalculated, and stored at each frequency. In addition, this method does not give information on improving the performance of the analysed structure [35].

2.3 Modal Damping

A modally decoupled generalised damping matrix $\mathbf{C_{gen}} \in \mathbb{R}^{a \times a}$, for structural behaviour, is made with the chosen a modal damping ratio D_a for the first a structural mode [36].

$$\mathbf{C_{gen}} = \mathbf{\Phi}^{\mathrm{T}} \mathbf{C} \mathbf{\Phi} \begin{bmatrix} c_{gen,1} & \cdots & 0 \\ \vdots & \ddots & \vdots \\ 0 & \cdots & c_{gen,a} \end{bmatrix} \tag{6}$$

in which, $c_{gen,a} = 2D_a k_{gen,a}$ is the mode a imaginary generalised stiffness and the modal matrix $\mathbf{\Phi} \in \mathbb{R}^{a \times n}$ containing first a real modes $\mathbf{\varphi_a}$ of the neighbouring undamped system. This imaginary generalised stiffness is a part of the generalised complex stiffness $k_{gen,a}^c = k_{gen,a} + i c_{gen,a}$.

$\mathbf{C}$ which is the imaginary complex stiffness system matrix can be obtained as follows:

$$\mathbf{C} = \mathbf{M} \left(\sum_1^a \frac{2 D_a \omega_{0,a}^2}{m_{gen,a}} \mathbf{\varphi_a} \mathbf{\varphi_a}^{\mathrm{T}} \right) \mathbf{M} \tag{7}$$

where m_{gen} is the generalised mass.

There is a very important difference of modal damping with other models previously discussed, as in this model damping in a structure is distributed with respect to modal damping ratios of specific mode shape at specific frequencies. Due to this unclear distribution, it is almost impossible to predict where damping is located in the structure. Also, only the a modes that are considered in the modal damping ratio are damped while the others remain undamped. As modal damping relies on the system and mathematical specification (uncondensed damping matrix), it is not truly physical. [35, 37].

3. Proposed model – Multi DOFs FEA Implementation

In the present work, we elaborate on the non-linear hysteretic damping model by Spitas et al. [32], which produces for time-domain solutions a largely frequency insensitive hysteretic behaviour, consistent with the behaviour of several engineering materials, such as metal alloys. This has the form:

$$f = \mathbf{K}\mathbf{u} + \frac{\mathbf{C}}{u^*} \dot{\mathbf{u}} \tag{8}$$

where $\mathbf{C}$ is a constant and the added term u^* is a special function of $\mathbf{u}$ (the current local state) and its derivatives calculated using the prior state history by way of backward differences.

The term u^* is an instantaneous correction factor, based on the local approximation of the system's response as an elementary harmonic oscillation within a sufficiently small interval $[t, t+\delta t]$.

$$u(t) = \tilde{u} \sin(\omega t + \theta) \qquad t \in [t, t+\delta t] \tag{9}$$

where ω is the instantaneous frequency of said approximation. With Eq. 9 having three parameters, for an infinitesimal interval $\delta t \to 0$, the approximation becomes exact up to and including the 2nd derivative. Obviously, ω becomes equal to the steady-state frequency of a damped vibration under harmonic excitation. Using Eq. 9, we can derive that:

$$\frac{\frac{d^2}{dt^2}\mathbf{u}}{\mathbf{u}} = -\omega^2 \tag{10}$$

From Eq. 10 it is, therefore, possible to estimate $u^* = \sqrt{(d^2\mathbf{u}/dt^2)/\mathbf{u}}$. At each time step of a dynamical simulation, this factor is computed using the immediately known prior state, which is the displacement response and its backward time differences. This is a simple and mathematically robust computation, except for those instances when $\mathbf{u} \to 0$, which gives rise to singularities in the estimator function. More details of this derivation are discussed at length in [45].

If we set $\mathbf{C}^{\bullet} = \mathbf{C}/u^*$ and recalculate $\mathbf{C}^{\bullet}$ at every time step, the model becomes:

$$f = \mathbf{K}\mathbf{u} + \mathbf{C}^{\bullet}\dot{\mathbf{u}} \tag{11}$$

which in computational terms is identical to the conventional Kelvin-Voigt model, but with the important difference that at each new time step and the local value $\mathbf{C}^{\bullet}$ is constantly re-computed in the present model.

The conventional Kelvin model is accomplished using the damping coefficient β. An approximate characterization of β is equivalent to two times the damping ratio; $\beta = 2\,(\zeta)$, which is equivalent to the loss factor $g = 2\,(\zeta)$, where ζ is the damping ratio. In a modal decoupled dynamic system $\beta_i = 2\,(\zeta_i/\omega_i)$, where the subscript i denotes the ith eigenmode [27]. In non-decoupled dynamic analysis, situations ω_i is set to 1.0 as an approximation, yielding $\beta_i = 2(\zeta)$. The damping matrix then is formed using β as the stiffness matrix multiplier,

$$\mathbf{C} = \beta \mathbf{K} \tag{12}$$

By recasting the stiffness matrix multiplier β as in Eq. 11, the desired modified hysteresis damping model is achieved:

$$\mathbf{C}^{\boldsymbol{\cdot}} = \frac{\beta \mathbf{K}}{u^{\boldsymbol{\cdot}}} \tag{13}$$

Beyond Eq. 10, other higher-order estimators of ω are possible, such as $\sqrt{(d^3\mathbf{u}/dt^3)/(d\mathbf{u}/dt)}$. As with the previous estimator, this is also susceptible to singularities when $d\mathbf{u}/dt \to 0$ therefore in this work we use both estimators in conjunction by defining the function $u^{\boldsymbol{\cdot}}$ in Eq. 8 as follows:

$$u^{\boldsymbol{\cdot}} = \sqrt{\min\left(\left|\frac{d^3\mathbf{u}}{dt^3}/\frac{d\mathbf{u}}{dt}\right|, \left|\frac{d^2\mathbf{u}}{dt}/\mathbf{u}\right|\right)} \tag{14}$$

where the min(…) function serves to eliminate either of the terms $|(d^3\mathbf{u}/dt^3)/(d\mathbf{u}/dt)|, |(d^2\mathbf{u}/dt^2)/\mathbf{u}|$ when a singularity condition emerges, to reduce undesired artefacts.

Therefore, the EOM is finally written in the form:

$$f = \mathbf{K}\mathbf{u} + \frac{\beta}{u^{\boldsymbol{\cdot}}}\mathbf{K}\dot{\mathbf{u}} + \mathbf{M}\ddot{\mathbf{u}} \tag{15}$$

The terms $d^3\mathbf{u}/dt^3$ and $d^2\mathbf{u}/dt^2$ appearing in Eq. 14 are evaluated numerically based on the immediately prior time history of the local solution, by means of backward differences, as follows: Denoting the displacement at current and previous three-time steps by $u_i, u_{i-1}, u_{i-2},$ and u_{i-3}, and assuming a constant time step h, the backward finite difference formulas used are presented in Eqs. 16 – 18.

$$\frac{d\mathbf{u}}{dt} \approx \frac{u_i - u_{i-1}}{h} \tag{16}$$

$$\frac{d^2\mathbf{u}}{dt} \approx \frac{u_i - 2u_{i-1} + u_{i-2}}{h^2} \tag{17}$$

$$\frac{d^3\mathbf{u}}{dt^3} \approx \frac{u_i - 3u_{i-1} + 3u_{i-2} - u_{i-3}}{h^3} \tag{18}$$

At the beginning of a simulation, if it is not possible to have sufficiently informed initial conditions (up to the 3rd order time derivative), it follows that the initially predicted hysteretic response based on Eq. 14 will be sensitive to whatever default value will be used for the higher-order derivatives. However, we have confirmed that this is eliminated very quickly into the simulation, as regardless of the choice of these derivatives, the predicted behaviour is convergent.

Inspecting the time derivative ratios in Eq. 14, it can be noticed that if $\mathbf{u}$ were to follow a harmonic law (e.g. under the influence of a harmonic external excitation under steady-state) the ratios under the square root would both yield the instantaneous circular frequency of said harmonic oscillation. Denoting the instantaneous frequency of oscillation as ω we would observe that $u^{\boldsymbol{\cdot}} = \omega$. Therefore, in such a sub-case we may expect the present time-domain model to yield similar predictions as frequency-domain methods, such as those employing a complex stiffness; this is confirmed in the results that follow.

We point out that in the particular case of steady-state forced harmonic external excitation this method gives a nearly frequency-independent hysteresis response. Consequently, the forcing frequency is equivalent to the calculated instantaneous frequency correction factor of the present model, which agrees with the solution proposed by Neumark [38] on an original model by Bishop and the hysteretic model developed by Kussner [39-40] and Bishop [9-10, 41]. This is also consistent with the experimental results shown by Kimball and Lovell [8] that under changing harmonic excitation the loss factor stays almost constant. However, the present model has not been built upon any assumption of steady-state or harmonic motion, but instead on an instantaneous approximation that is reasonably valid under any kind of motion. Furthermore, unlike the aforementioned models, which are not suited to studying free vibrations or transient vibrations, the present model makes no assumptions that limit its applicability to these.

Table 1: Beam material properties

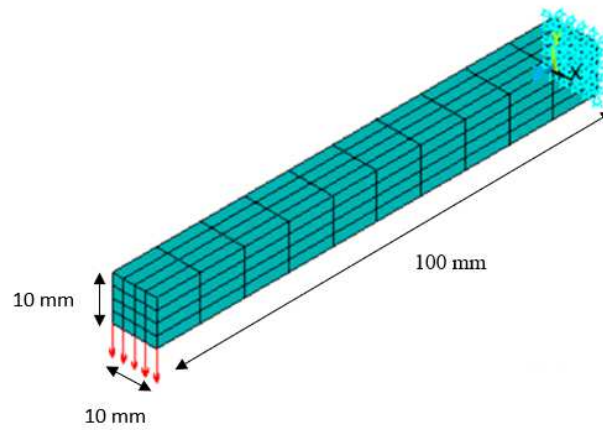| Material properties – Aluminium 2024	
Modulus of elasticity	$73.1 \times 10^9 \ N/m^2$
Density, ρ	$2780 \, kg/m^3$
Poisson ratio, γ	0.33
Tensile yield, S_y	$250 \times 10^6 \ N/m^2$
Tensile ultimate, S_u	$400 \times 10^6 \ N/m^2$
Beta damping, β	1×10^{-4} *(Typical loss factor of an aluminium bar with damp ratio ~ 0.005%)*

Fig. 1: Cantilever Beam Element Plot

4. Results and Discussion

4.1 Case study 1 – cantilever beam

4.1.1 *System geometry and topology*

A simple cantilever beam model is used in the study of hysteretic damping using different models. An aluminium cantilever beam of length 100 mm and 10 mm x 10 mm square cross-section is used for the analyses (Table1). The element plot of the beam model is shown in Fig. 1. A load of 9.81N is applied at the free end of the beam as a harmonic excitation force.

4.1.2 *Beam Simulations*

For the simulation, the cantilever beam (Fig. 1) is considered to study the behaviour of the proposed damping model on the dynamic response and compared it to the standard Kelvin-Voigt damping model.

Two different damping cases are studied here through harmonic sweep analysis. The first case employs the formulation that closely represents the modified hysteretic formulation in the transient analysis (time-domain). The second is the standard Kelvin-Voigt damping model which uses a stiffness matrix multiplier β to form the damping matrix. As outlined in section 3, the multiplier β is roughly equivalent to the loss factor $g = 2$ (ζ), where ζ is the damping ratio. In both cases, the harmonic response sweep is performed with the same 9.81 N load as shown in Fig. 1.

Introducing damping in a structural dynamic analysis. The damping matrix expression is reproduced as shown in Eq. 19 [42].

$$\mathbf{C} = \propto \mathbf{M} + (\beta + \beta_c)\mathbf{K} + \sum_{j=1}^{N_m}[(\beta_j^m + \frac{2}{\omega_e}\beta_j^\zeta)\mathbf{K_j}] + \sum_{k=1}^{N_e}\mathbf{C_k} + \mathbf{C_\zeta} \tag{19}$$

in which,

ω_e = excitation frequency in a harmonic analysis

$\mathbf{K_j}$ = stiffness matrix of element j

$\mathbf{C_k}$ = damping matrix of element

$\mathbf{C_\zeta}$ = frequency-dependent matrix

where the first term in the expression applies a multiplying factor α on the mass matrix **M** contributing to the damping matrix **C**. In the second and third terms, factors $\beta, \beta_c, \beta_j^m$ and β_j^ζ, all apply as multiplying factors on the stiffness matrix **K**; contributing to the damping matrix.

In general, factor β is used for modelling material-dependent damping in a structural system. Different β values can be applied to different parts of a structure using the factor β_j^m. For the hysteretic damping model development in the current research, the factor β_j^m is adjusted as shown in Eq. 13 to arrive at the multiplying factor $\mathbf{C}^*$.

Now, let's consider the formulation that closely represents the explicit hysteretic formulation. In Eq. 19 the third term $(2/\omega_e)\beta_j^\zeta$ $\mathbf{K_j}$ applies a constant damping ratio over the excitation frequency range. The damping ratio ζ to be applied is input through the material property command. This damping ratio input specification via the material property command allows specifying different damping ratio values ζ over different parts of a structure. With the supplied ζ the **K** matrix multiplier used in the damping matrix contribution is $(2\zeta/\omega_e)$.

With stepwise loading, the response plot with constant damping ratio is presented in Fig. 2. The **K**-matrix multiplying factor is (β/ω_e) since the damping factor used is $\beta_j^\zeta = \beta/2$. In other words, the metal hysteresis effect is already properly reproduced in the frequency domain by the complex stiffness model, which is a standard feature in ANSYS and other commercial software implementations.

In the Kelvin-Voigt model, the **K** matrix multiplier used is β for the damping matrix contribution in Eq. 19. After the computation of the model, harmonic sweep analysis is carried out and the response plot is obtained shown in Fig. 3.

Reviewing the response plots from Fig. 2-3, the Kelvin-Voigt model essentially damps out the displacement response of the modes higher than the constant damping ratio model. Also, it can be observed that at the first resonance the constant damping ratio model response shows higher displacement amplitudes than the Kelvin-Voigt damping model, i.e. the damping is lower when compared with the Kelvin-Voigt model response.

Additional results for the first four eigenmodes of the cantilever beam are shown in Fig. 4. It can be seen that the first four modes are bending modes in orthogonal directions. Note that the eigenmodes are in pairs as the beam cross-section is symmetric about two orthogonal axes.
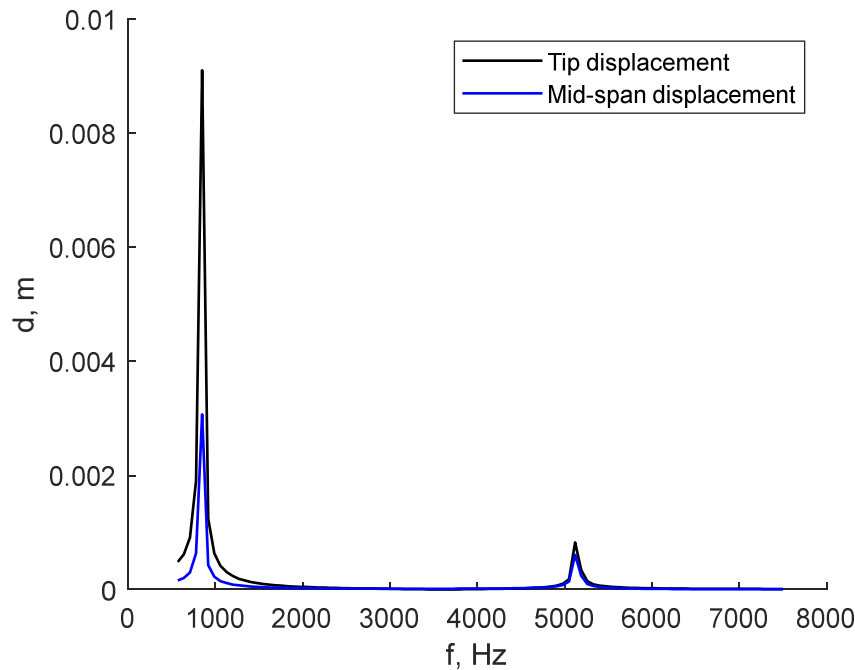
Fig. 2: Frequency Response - Stepwise Loading – Constant damping ratio model ($\left(2/\omega_e\right)\beta_j^\varsigma$ – Damping Factor)
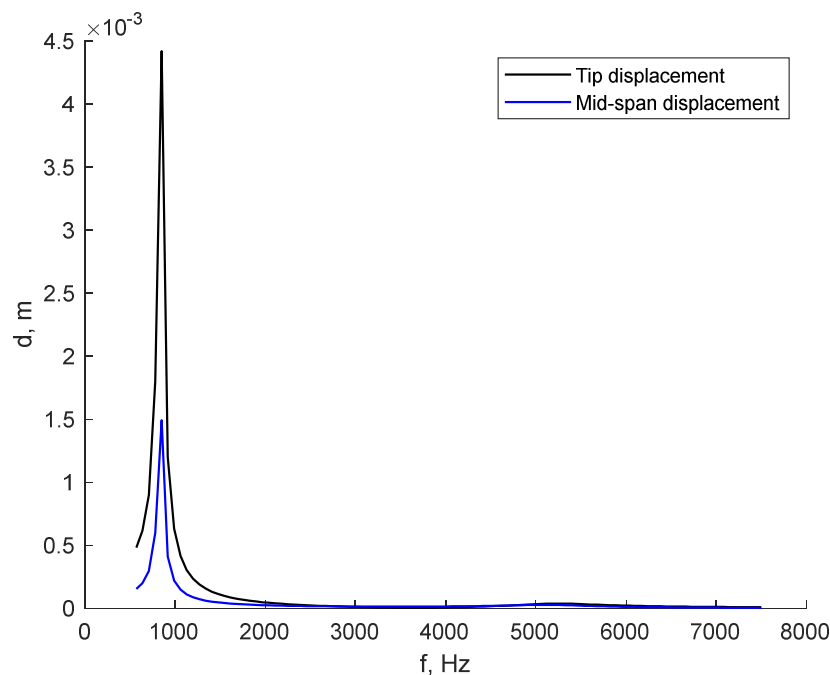

**Fig. 3:** Frequency Response - Stepwise Loading – Kelvin-Voigt Model (β damping model)

To confirm the frequency domain results, a time transient analysis of the cantilever beam is performed with the proposed model implemented for the time-domain analysis. Currently, in the time domain, there is no such model that can reproduce the hysteresis effect properly, hence the proposed model is introduced. To calculate the instantaneous oscillation frequency ω, that is used in updating the damping applied at each time step. At each time step, the displacement response from three previous time steps is read in from the results file. Backward finite difference formulas in Eqs. 16-18 are used in calculating the time derivatives, which are then used in Eq. 14. This novel model is expected to represent a more suitable response in the time-domain for structural dynamic applications than the conventional Kelvin-Voigt model.

The force loading of Fy=9.81 N (Fig. 1) is the initial condition applied over a time interval of 0.001 sec, roughly a single cycle period of the beam first resonant frequency. The applied loading is removed step-wise at 0.001 sec and the beam is allowed to undergo free oscillations. A beta damping value of β=1.0E-4 is used. So, in the transient solutions, the **K** matrix multiplying factor applied to the two material regions of the beam is β/ω_1, and β/ω_2. It is worthwhile to note that the local oscillation frequency values are roughly near the first resonant frequency of the beam, as one would expect. The wide variations that occur at certain time points may be attributed to the numerical evaluations at or near an inflexion point on the oscillation curve.
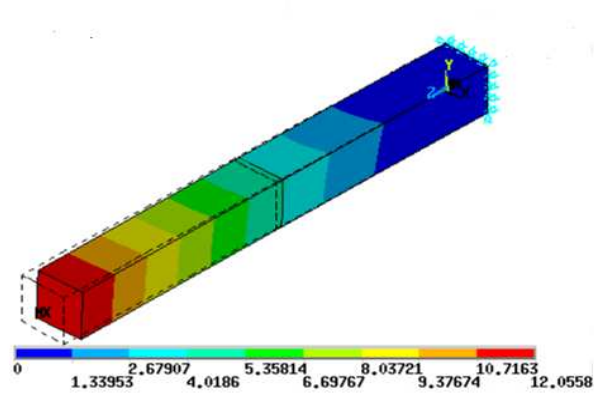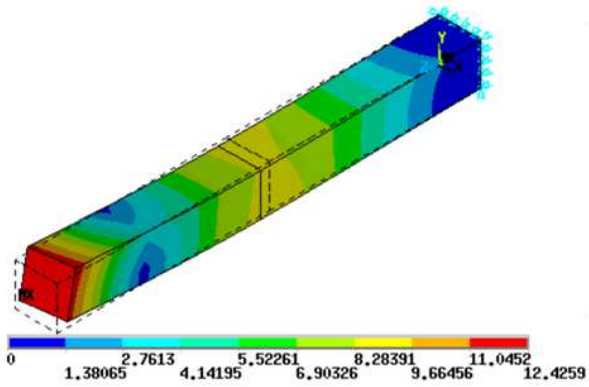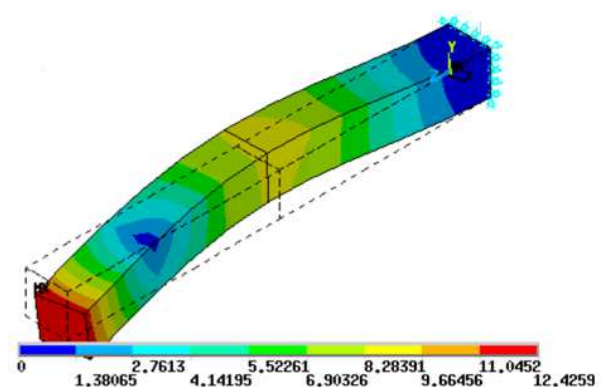
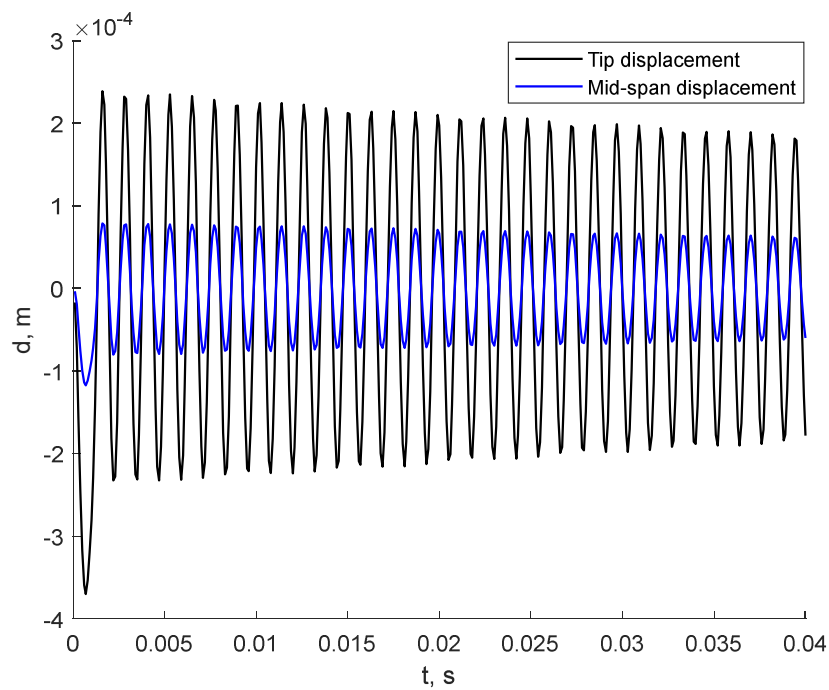(a) Mode 1 – 838 Hz
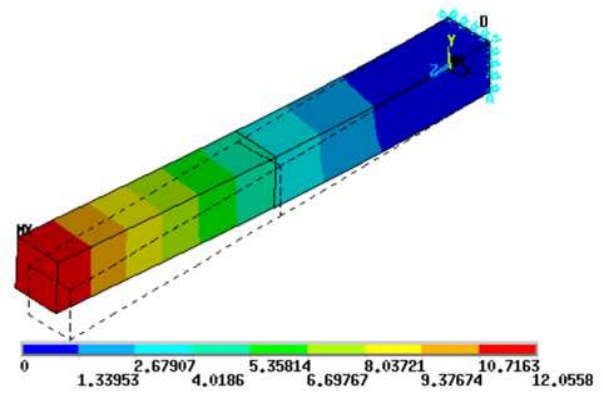
(b) Mode 2 – 838 Hz

(c) Mode 3 – 5140 Hz

(d) Mode 4 – 5140 Hz

Fig. 4: First four eigenmodes of the cantilever beam

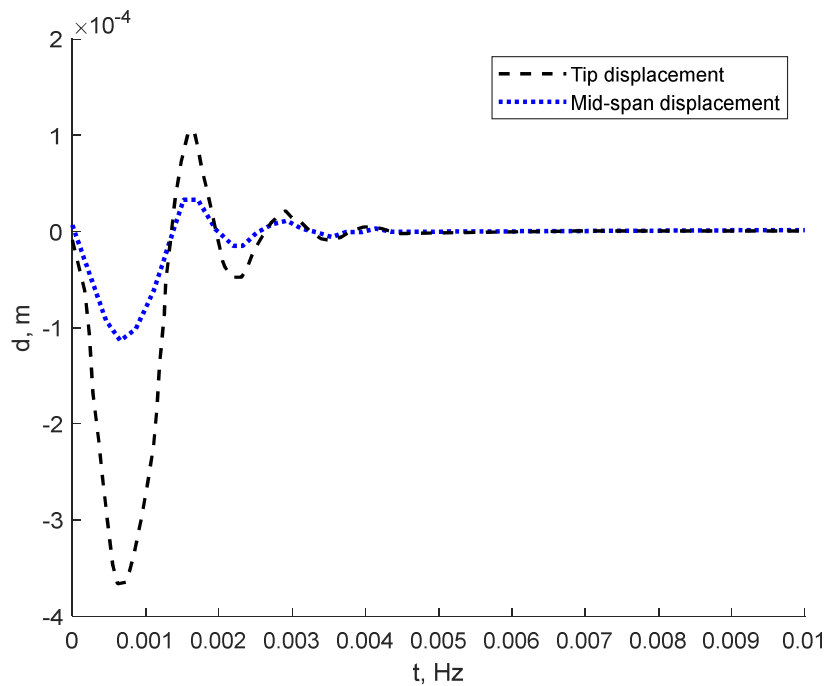**Fig. 5:** Response with modified damping model (initial load of Fy= 9.81 N applied over 1/1000 sec and released) β=1.0E-4

Fig. 6: Response with beta damping model (initial load of Fy= 9.81 N applied over 1/1000 sec and released) β=1.0E-4

The transient response plot of the beam displacement over a period of 0.04s and 0.01s is shown in Fig. 5. The tip and mid-span displacements are gradually decreasing under the influence of damping. The decaying vibration amplitude due to damping is noticeable in the longer duration plot with T = 0.04 s. Presented in Fig. 6 is the transient response plot with the Kelvin-Voigt model (beta damping model). For this damping model, the effect of damping is much more pronounced than the proposed model. The model predicts that the beam stops oscillating after about 0.005s in the Kelvin-Voigt model, while the oscillations continue and diminish at a much slower rate in the modified hysteretic damping model, showing more realistic damping behaviour of the material. This confirms the harmonic sweep results in the frequency domain.

The main difference between the beta damping model and the proposed model is the **K** matrix multiplication factor used in the formation of the damping matrix, **C**, which is β in the beta-damping model and $\beta \times (1/\omega)$ in the proposed model. Since ω in this free oscillation problem is of the order of the first eigenfrequency, 838.36 Hz, much lower damping is applied in the modified hysteretic damping model, resulting in the oscillations to sustain longer than the beta damping model.

4.2 Case Study 2 - Multi-Material Structures

This case study is done to confirm if the proposed non-linear hysteresis damping formulation shows a similar trend obtained in section 4.1 when applied to other systems with different geometry and topology.

4.2.1 System geometry and topology

In this case study, a multi-structured cantilever beam is used in validating the modified hysteretic damping formulation in section 3.

A bimetallic cantilever beam of length 100 mm and 10 mm x 10 mm square cross-section is used in the analyses. The bimetallic beam square cross-section is made up of 10 mm x 5 mm aluminium and 10 mm x 5 mm copper. The material properties used are shown in Table 2. An element plot of the bimetallic beam is shown in Fig. 7. The top half of the beam thickness in the Y-direction is aluminium 2024, and the bottom half is copper.

4.2.2 Bimetallic Beam Simulations

The displacement response of the constant damping ratio model under a tip load of 9.81 N is presented in Fig. 8. This response will then be compared to the proposed transient formulation response (like in section 4.1.2), to confirm if the proposed formulation gives a more appropriate response when compared to the conventional model.

In the Kelvin-Voigt model, the **K** matrix multiplier used is replaced with the β in Eq. 19, like in the previous case study. A harmonic sweep analysis is performed and the response plot is obtained shown in Fig. 9.

Table 2: Beam material properties

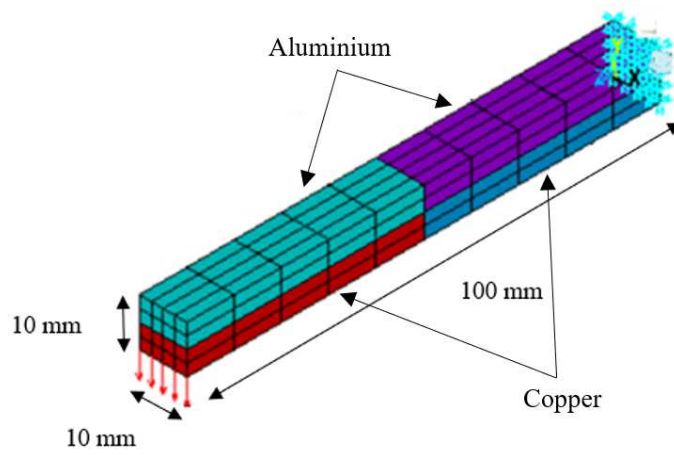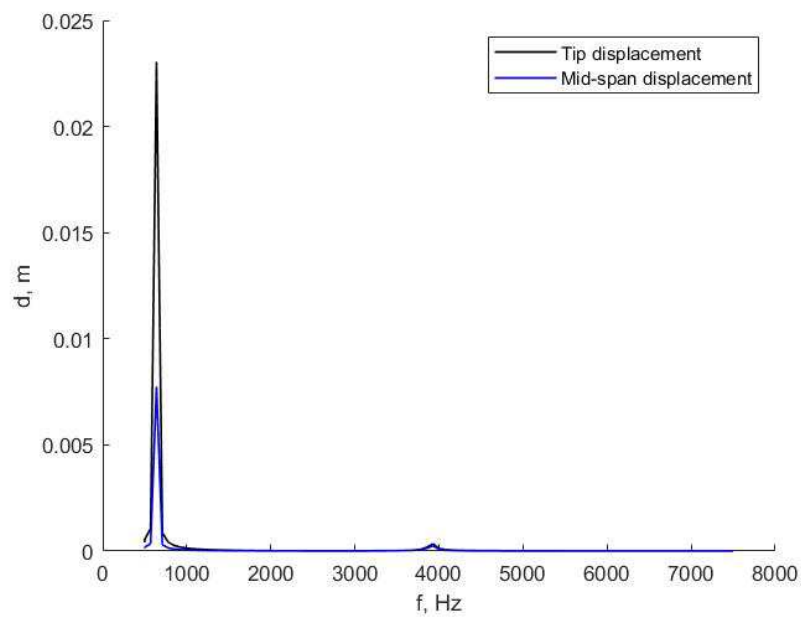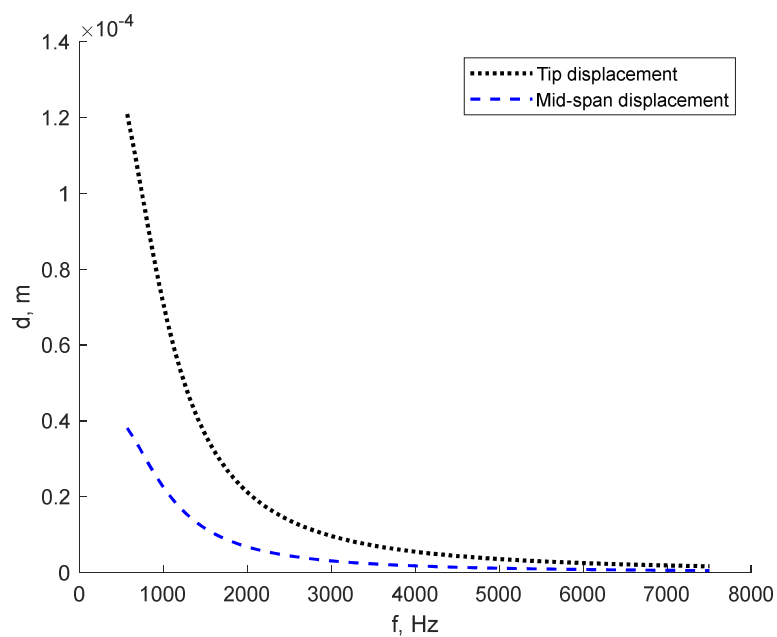| Material properties	Copper	Aluminium 2024
Modulus of elasticity	$110 \times 10^9 \ N/m^2$	$73.1 \times 10^9 \ N/m^2$
Density, ρ	$8930 \ kg/m^3$	$2780 \ kg/m^3$
Poisson ratio, γ	0.34	0.33
Tensile yield, S_y	$33.3 \times 10^6 \ N/m^2$	$250 \times 10^6 \ N/m^2$
Tensile ultimate, S_u	$210 \times 10^6 \ N/m^2$	$400 \times 10^6 \ N/m^2$
Beta damping, β	2×10^{-3}	1×10^{-4}

Fig. 7: Bimetallic beam elements plot

Fig. 8: Bimetallic beam frequency response - Stepwise loading – Constant damping ratio model ($(2 / \omega_e)\beta_j^c$ – Damping Factor)

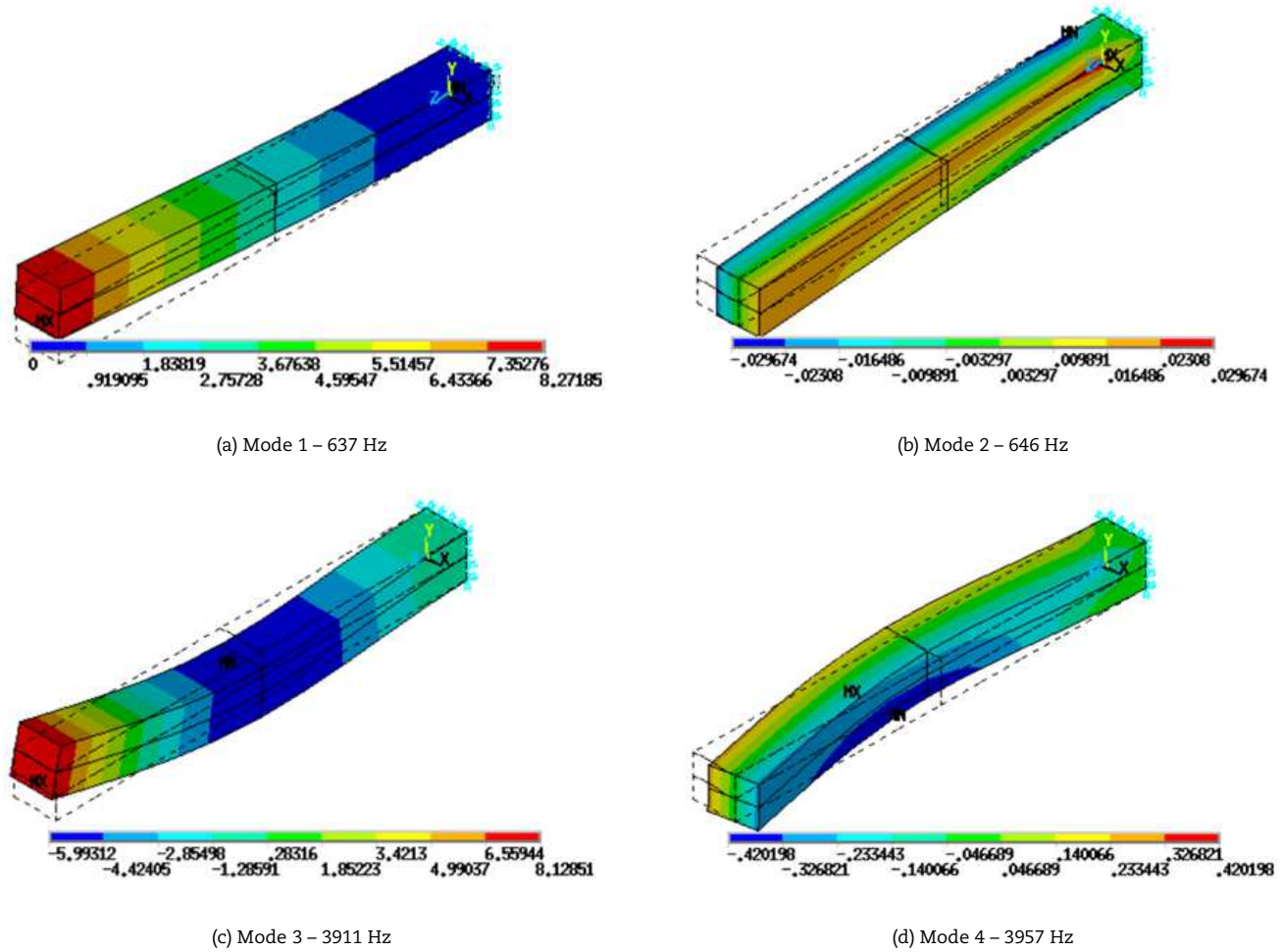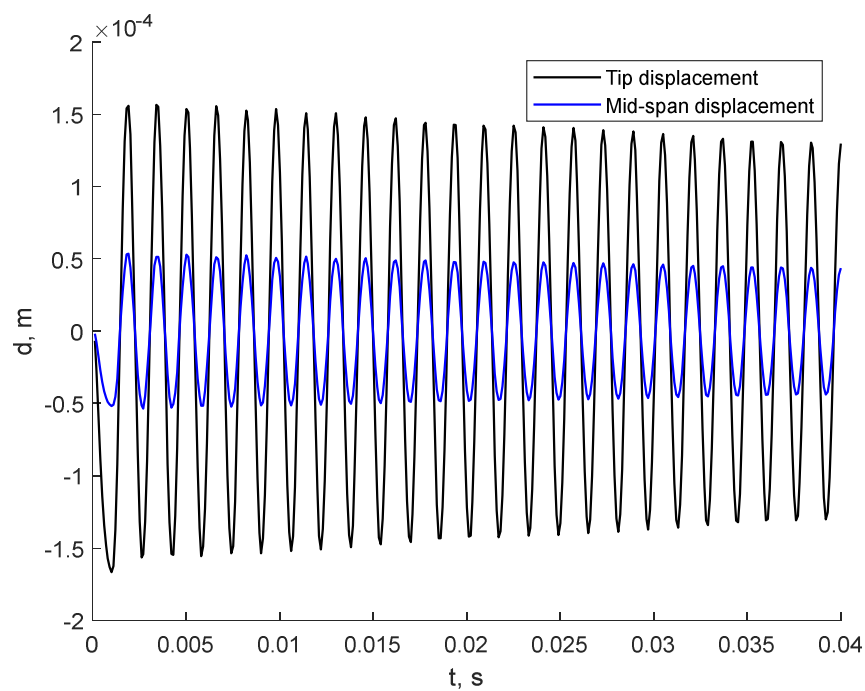**Fig. 9:** Bimetallic beam frequency response - Stepwise loading – Kelvin-Voigt Model (β damping model)

(a) Mode 1 – 637 Hz

(b) Mode 2 – 646 Hz

(c) Mode 3 – 3911 Hz

(d) Mode 4 – 3957 Hz

Fig. 10: Bimetallic beam first four eigenmodes

Fig. 11: Bimetallic beam Response with modified damping model (initial load of Fy= 9.81 N applied over 1/1000 sec and released) β=1.0E-4

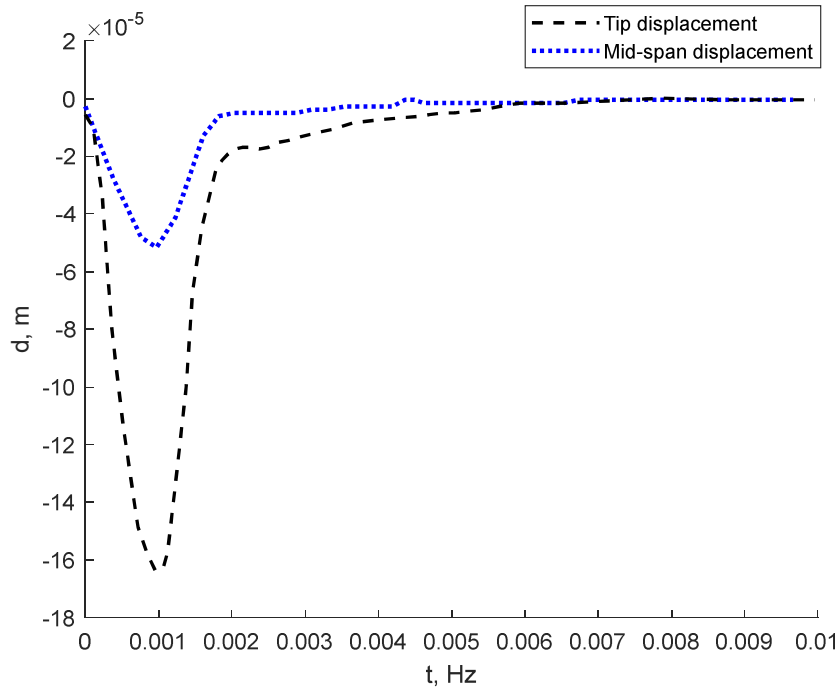**Fig. 12:** Bimetallic beam response with β damping model (initial load of Fy= 9.81 N applied over 1/1000 sec and released) β=1.0E-4

Reviewing the dynamic response results, overall, the Kelvin-Voigt damping model introduces much higher damping than the explicit hysteretic damping model. The response results are similar to the previous case study, which shows that even the in-built function (constant damping ratio model) in the frequency domain does present more appropriate damping behaviour than the conventional Kelvin-Voigt model.

Additional results on the first four eigenmodes are displayed in Fig. 10. The first four modes are bending modes in orthogonal directions.

Further verification of the modified model is carried out through transient analysis of the bimetallic beam. The force loading of Fy=9.81 N at the beam tip is the initial condition applied over a time interval of 0.001s, roughly a single cycle period of the beam first resonant frequency. The applied loading is removed step-wise at 0.001s and the bimetallic beam is allowed to undergo free oscillations. Beta damping values of β=1.0E-4 and β=2.0E-3 for aluminium and copper are used, respectively. In the transient solutions, the **K** matrix multiplying factor applied to the four material regions of the bimetallic beam is β/ω_1 , β/ω_2 , β/ω_3 and β/ω_4 .

The transient response of the bimetallic beam with a modified non-linear hysteretic damping model is shown in Fig. 11. Under the same initial loading conditions, the transient response was obtained for the Kelvin-Voigt model (beta damping model) displayed in Fig. 12.

The results are similar to the cantilever beam case study in section 4.1, in which the Kelvin-Voigt damping model (Fig. 12) shows the effect of damping that is much more pronounced than the modified hysteretic damping model (Fig. 11). In the conventional model, the beam stops oscillating after about 0.006s (suggesting overdamping), while in the proposed model the oscillation continues and diminishes at a much slower rate which should be the case for metallic materials. These results agree with the frequency domain responses, the proposed model represents the standard constant damping ratio, while the Kelvin-Voigt model is the beta damping model.

5. Conclusion

The current paper introduces a finite element MDOF hysteresis model that is based on its instantaneous state under forced vibration that does not require prior knowledge of the history of motion, excitation characteristics and frequency. The damping behaviour is analysed through two case studies of a single- and bi-metal beam in the frequency domain (constant damping ratio model vs. Kelvin-Voigt/beta-damping model) and time-domain (MDOF hysteresis model vs. Kelvin-Voigt/beta-damping model). The results illustrate that in the frequency domain the beta-damping model damps out the displacement response of the modes more than the constant damping ratio model (the frequency-domain equivalent of the proposed model). Similarly, in the time-domain analysis, the beta-damping model displayed unnatural rapid damping for both single- and bi-metal beam, compared to the proposed MDOF hysteresis model. The solutions obtained from the proposed model exhibited largely frequency insensitive hysteretic behaviour, consistent with the behaviour of several engineering materials.

Author Contributions

H.B. Tariq has written, edited and simulated results in the manuscript; C. Rajakumar edited manuscript and simulated and analysed results; D. Zhang analysed results, C. Spitas planned the scheme, initiated the project, and suggested the analysis. The manuscript was written through the contribution of all authors. All authors discussed the results, reviewed, and approved the final version of the manuscript.

Conflict of Interest

The authors declared no potential conflicts of interest with respect to the research, authorship, and publication of this article.

Funding

References

[1]   Ding, Z., Li, L., Hu, Y., Li, X., Deng, W., State-space based time integration method for structural systems involving multiple nonviscous damping models, *Computers & Structures*, 171, 2016, 31-45.

[2]   Chopra, A., *Dynamics of Structures*, 4th ed. Pearson, 2011.

[3]   Lakes, R., Materials with structural hierarchy, *Nature*, 361, 1993, 511–515.

[4]   Huang, Y., Sturt, R., Willford, M., A damping model for nonlinear dynamic analysis providing uniform damping over a frequency range, *Computers & Structures*, 212, 2019, 101-109.

[5]   Lazan, B., *Damping of materials and members in structural mechanics*, Oxford Pergamon Press, New York, 1968.

[6]   Maia, N., Reflections on the Hysteretic Damping Model, *Shock and Vibration*, 16(5), 2009, 529-542.

[7]   Humar, J., *Dynamics of Structures*, 3rd ed. CRC Press, 2012.

[8]   Kimball, A., Lovell, D., Internal Friction in Solids, *Physical Review*, 30(6), 1927, 948-959.

[9]   Bishop, R., The Treatment of Damping Forces in Vibration Theory, *The Journal of the Royal Aeronautical Society*, 59, 1955, 738-742.

[10] Bishop, R., Johnson, D., *The mechanics of vibration*, Cambridge University Press, Cambridge, 1960.

[11] Caughey, T., Vibration of dynamic systems with linear hysteretic damping, *ASME*, New York 1962.

[12] Crandall, S., The role of damping in vibration theory, *Journal of Sound and Vibration*, 11(1), 1970, 3-18.

[13] Reid, T., Free Vibration and Hysteretic Damping, *The Journal of the Royal Aeronautical Society*, 60(544), 1956, 283.

[14] Fraijs, V., *Influence of internal damping on aircraft resonance*, AGARD, 1960.

[15] Crandall, S., The Hysteretic Damping Model in Vibration Theory, *Proceedings of the Institution of Mechanical Engineers, Part C: Mechanical Engineering Science*, 205(1), 1991, 23-28.

[16] Makris, N., Causal Hysteretic Element, *Journal of Engineering Mechanics*, 123(11), 1997, 1209-1214.

[17] Adhikari, S., Wagner, N., Direct time-domain integration method for exponentially damped linear systems, *Computers & Structures*, 82(29-30), 2004, 2453-2461.

[18] Cortés, F., Mateos, M., Elejabarrieta, M., A direct integration formulation for exponentially damped structural systems, *Computers & Structures*, 87(5-6), 2009, 391-394.

[19] Adhikari, S., *Damping models for structural vibration*, PhD thesis, Cambridge University, 2000.

[20] Soroushian, A., A General Rule for the Influence of Physical Damping on the Numerical Stability of Time Integration Analysis, *Journal of Applied and Computational Mechanics*, 4(5), 2018, 467-481.

[21] Inaudi, J., Kelly, J., Linear Hysteretic Damping and the Hilbert Transform, *Journal of Engineering Mechanics*, 121(5), 1995, 626-632.

[22] Muravskii, G., On frequency independent damping, *Journal of Sound and Vibration*, 274, 2004, 653–668.

[23] Muravskii, G., Linear models with nearly frequency independent complex stiffness leading to causal behavior in time domain, *Earthquake Engineering & Structure Dynamics*, 33, 2006, 13–33.

[24] Scanlan, R., Linear damping models and causality in vibrations, *Journal of Sound and Vibration*, 13(4), 1970, 499-503.

[25] Sanliturk, K., Koruk, H., Development and validation of a composite finite element with damping capability, *Composite Structures*, 97, 2013, 136-146.

[26] Cortés, F., Elejabarrieta, M., An approximate numerical method for the complex eigenproblem in systems characterised by a structural damping matrix, *Journal of Sound and Vibration*, 296(1-2), 2006, 166-182.

[27] Zhang, S., Chen, H., A study on the damping characteristics of laminated composites with integral viscoelastic layers, *Composite Structures*, 74(1), 2006, 63-69.

[28] Cortés, F., Elejabarrieta, M., Structural vibration of flexural beams with thick unconstrained layer damping, *International Journal of Solids and Structures*, 45(22-23), 2008, 5805-5813.

[29] Rao, M., Echempati, R., Nadella, S., Dynamic analysis and damping of composite structures embedded with viscoelastic layers, *Composites Part B: Engineering*, 28(5-6), 1997, 547-554.

[30] Zhang, S., Chen, H., A study on the damping characteristics of laminated composites with integral viscoelastic layers, *Composite Structures*, 74(1), 2006, 63-69.

[31] Plagianakos, T., Saravanos, D., Mechanics and finite elements for the damped dynamic characteristics of curvilinear laminates and composite shell structures, *Journal of Sound and Vibration*, 263(2), 2003, 399-414.

[32] Spitas, C., Dwaikat, MMS., Spitas, V., Non-linear modelling of elastic hysteretic damping in the time domain, *Archives of Mechanics*, 72(4), 2020, Rayleigh, L., Theory of Sound , Dover Publications, New York, 1945.

[33] Foss, K., Coordinates Which Uncouple the Equations of Motion in Damped Linear Dynamic Systems, *Journal of Applied Mechanics*, 25, 1958, 361-364.

[34] Johnson, C., Kienholzt, D., Finite Element Prediction of Damping in Structures with Constrained Viscoelastic Layers, *AIAA Journal*, 20(9), 1982, 1284-1290.

[35] Hoser, M., Boswald, M., Govers, Y., Validating Global Structural Damping Models for Dynamic Analyses, *Deutscher Luft- und Raumfahrtkongress*, 2015, 1-10.

[36] Rittweger, A., Dieker, S., Abdoly, K., Albus, J., Coupled Dynamic Load Analysis with different Component Damping of the Substructures, *International Astronautical Congress*, 2008.

[37] Neumark, S., Concept of complex Stiffness Applied to Problems of Oscillation with Viscous and Hysteretic Damping, *Aeronautical Research Council R&M*, 1962.

[38] Küssner, H., *Schwingungen von flugzeugflügeln*, Jahrbuch der Deutscher Versuchsanstalt für Luftfahrt, 1929, 319-320.

[39] Küssner, H., Augenblicklicher Entwicklungsstand der Frage des Flugelflatterns, *Luftfahrtforschung*, 12, 1935, 193.

[40] Bishop, R., The general theory of hysteretic damping, *The Aeronautical Quarterly*, 7(1), 1956, 60-70.

[41] ANSYS, Theory Reference for the Mechanical APDL and Mechanical Applications, ANSYS, 2009, 897-899.

ORCID iD

H.B. Tariq https://orcid.org/0000-0002-2166-7897
D. Zhang https://orcid.org/0000-0002-9253-4178